

# Enhanced Transmission by Periodic Hole Arrays in Metal Films

K. Milliman

University of Florida

July 30, 2008

## **Abstract**

Three different square periodic hole arrays were manufactured on a silver film in order to explore the dependence of transmittance intensity peaks on hole size, lattice spacing, and the refractive index of material above and below the silver film. The three arrays all had the same open area fraction of 10%. It was observed that the transmittance intensity was almost twice the open area fraction when the index of refraction for material above and below the substrate were almost equal ( $n=1.4$  and  $n=1.5$  respectively).

## Introduction

Periodic arrays exhibit surprising optical behavior in that the transmittance intensity peaks are larger than the open area fraction of the array [1]. The open area fraction,  $f$ , is the ratio of hole area to field area calculated by the equation,  $f=(a/D_g)^2$ , where  $a$  is the hole size and  $D_g$  is the lattice spacing (see Fig. 1).

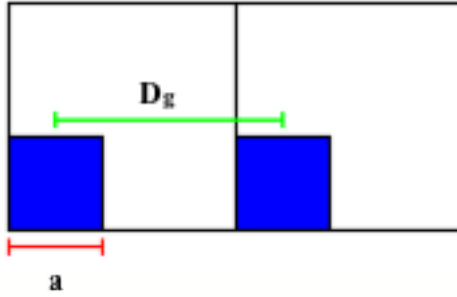


Figure 1: Sketch of holes displaying lattice spacing,  $D_g$ , and hole size,  $a$

These transmittance intensity peaks indicate that light incident on the metal surface, as well as light hitting the hole area, is transmitted to the output surface. These transmissions do not match the predictions made by classical electromagnetic theory [2], and multiple independent theories attempt to explain this phenomenon including coupled surface plasmon interactions and trapped electromagnetic modes. A surface plasmon is a collective excitation of electrons at the interface between a metal and an insulator. The theory states that, combined with a photon, a surface plasmon forms modes

on this interface, and given a periodic structure, these modes on the input and output sides can couple and transfer energy [3]. Trapped electromagnetic modes are long-lived quasi-stationary states that exist near structures and are assumed to be responsible for resonant transmissions by slowly decaying and emitting quasi-monochromatic radiation [3]. As the open area fraction of the film decreases or the holes become smaller, the trapped electromagnetic modes live longer [3, 4] .

For this project we analyzed how the wavelength peaks of the enhanced transmission depended on lattice spacing and hole size and investigated the influence of the refractive index of the media on either side of the metal film. The sample studied consisted of three periodic arrays manufactured on the same silver film on a fused silica substrate. All three arrays have the same open area fraction of 10%, but differ in hole size and spacing (see Table I).

Table I: Lattice spacing,  $D_g$ , and hole size,  $a$ , for each 100nm x 100nm array

Sample	$D_g$	$a$	Open Area Fraction, $f$
A	0.8 $\mu\text{m}$	253 nm	0.1
B	1.0 $\mu\text{m}$	316 nm	0.1
C	1.2 $\mu\text{m}$	379 nm	0.1

We investigated the influence that the refractive index of the medium on the upper side of the metal film has on the enhanced transmission using two materials: air and a positive polymer resist, polymethyl methacrylate (PMMA). Air has an index of refraction of 1, PMMA has an index of refrac-

tion of approximately 1.5 [5], and the refractive index for fused silica is 1.4 [6].

## Sample Preparation and Measurements

We deposited a 100 nm thick film of silver onto a fused silica substrate using thermal evaporation. We then spin-coated a layer of the PMMA and baked the sample on a hot plate at 180° C for one minute. We used electron beam lithography to pattern the square hole arrays onto the silver film. As a positive photoresist, the areas of PMMA exposed to the electron beam will become soluble to certain developing chemicals, while unexposed portions remain insoluble to the developers. The developing chemicals used were isopropanol and methyl isobutyl ketone (MIBK). We developed the sample until the periodic hole structure in the PMMA was visible under a microscope. We used a dry etching process to create the holes in the silver film by bombarding the sample with a beam of argon ions. Ions incident on the regions with no PMMA penetrated the silver film, while ions that struck PMMA did not affect the sample. After measuring transmittance and reflectance for this configuration of the sample, we removed the remaining PMMA using acetone and again measured transmittance and reflectance. Finally, we spin-coated PMMA over the entire area and baked the sample on a hot plate at 180° C and concluded our transmittance and reflectance measurements. These steps are illustrated in Fig. 2.

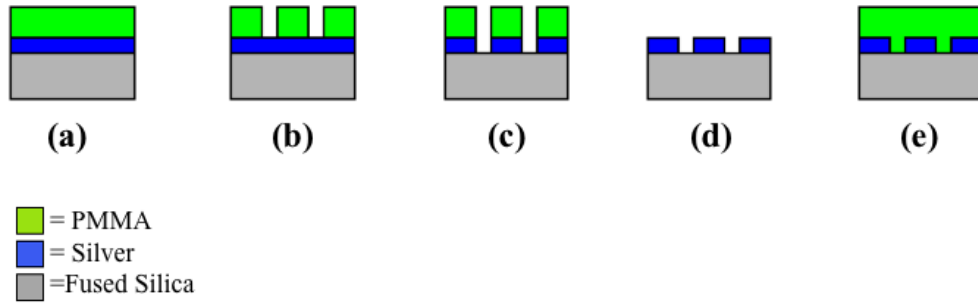


Figure 2: Sample preparation: (a) PMMA spin coated, (b) exposed PMMA dissolved away by developing chemicals, (c) holes etched by argon ions, (d) PMMA completely removed from sample, (e) PMMA spin coated over entire sample.

Our attempts to manufacture three other samples, two with gold metal film and one with silver, failed during the dry etching process. Graduate student Dimitrios Koukis is attempting to manufacture more samples using a different method that minimizes the amount of etching needed to complete the periodic hole arrays.

## Results and Discussion

We measured the intensity of transmittance and reflectance for each of the three arrays under three conditions. The first had PMMA layered on top of the remaining silver film (Fig. 2c); in the second all the PMMA was removed (Fig. 2d); and finally, a layer of PMMA was spin-coated over the

entire sample (Fig. 2e). The feature seen in Fig. 3 at  $\lambda = 326$  nm is the silver plasmon peak. As seen in Figs. 3, 4, and 5, the transmittance graphs show a very similar pattern of dips and peaks repeated for each sample occurring at different wavelengths. Sample A has the smallest hole size and closest lattice spacing and exhibits features at the shortest wavelengths, while sample C has the largest hole size and greatest lattice spacing exhibits features at the longest wavelengths. Also the transmittance peaked at approximately the same intensity for all samples under each condition: 0.056% for limited PMMA, 0.044% for no PMMA on the sample, and 0.19% for the entire sample covered with PMMA. For the last condition, the transmittance intensity peaked at almost twice the open area fraction. An exception to this is sample C when the sample was entirely covered in PMMA. Sample C had a peak transmittance intensity of approximately 0.14%, about 0.05% lower than sample A and sample B, but still greater than the open area fraction for the sample. The last condition had such an increase in transmittance peak because the index of refraction for PMMA ( $n=1.5$ ) is a closer match to the refractive index for the substrate material, fused silica ( $n=1.4$ ), than air ( $n=1$ ).

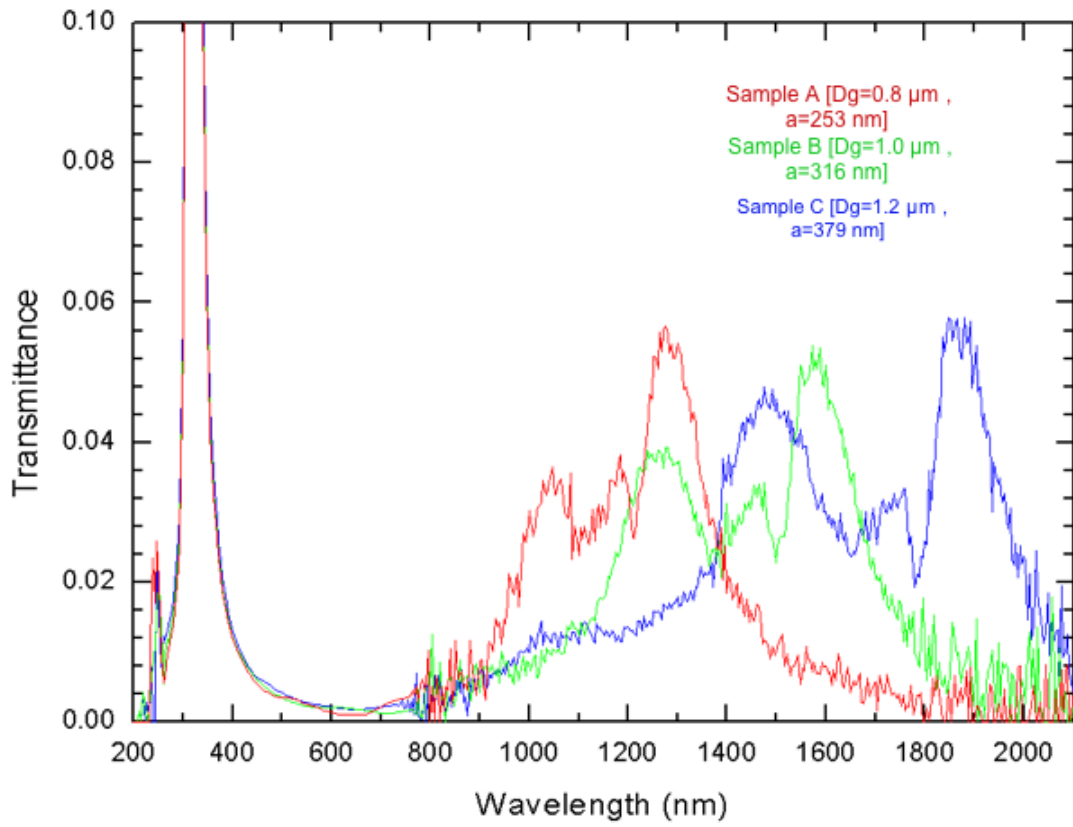


Figure 3: Transmittance intensity using 10x magnification for sample with PMMA on top of remaining silver film, Figure 2(c).

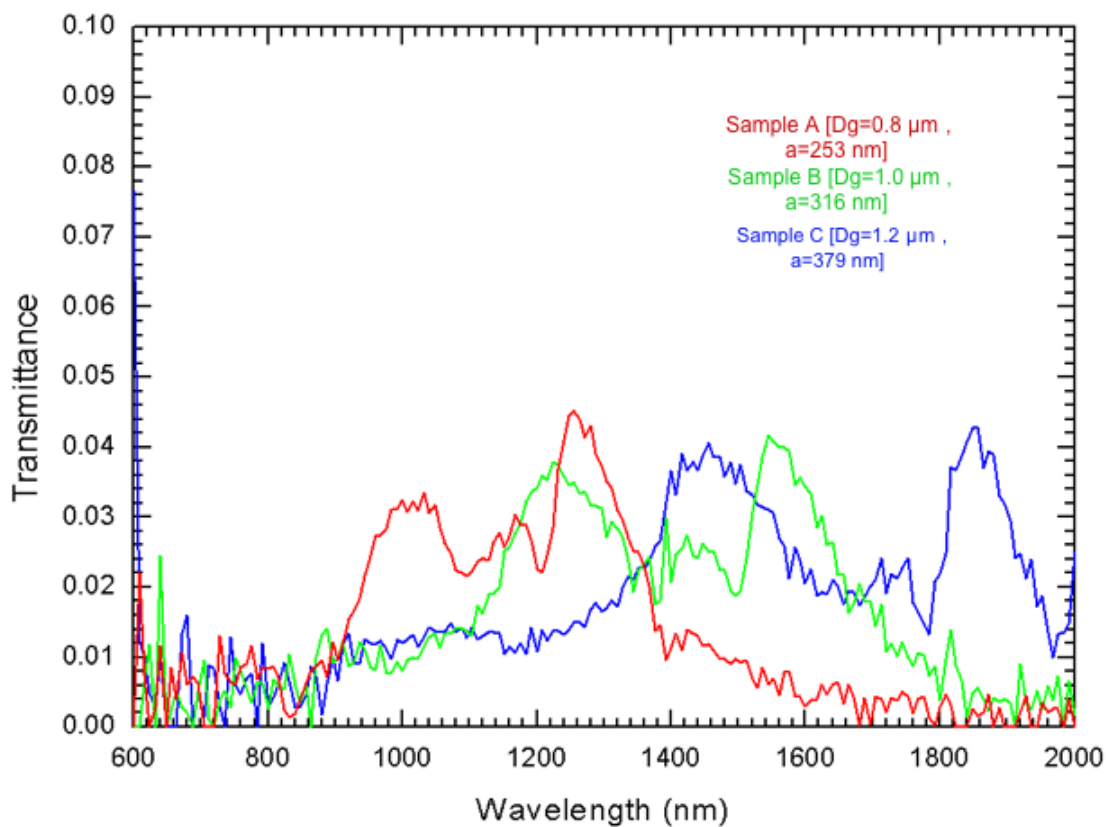


Figure 4: Transmittance intensity using 10x magnification of NIR wave-lengths for sample with no PMMA, Figure 2(d).

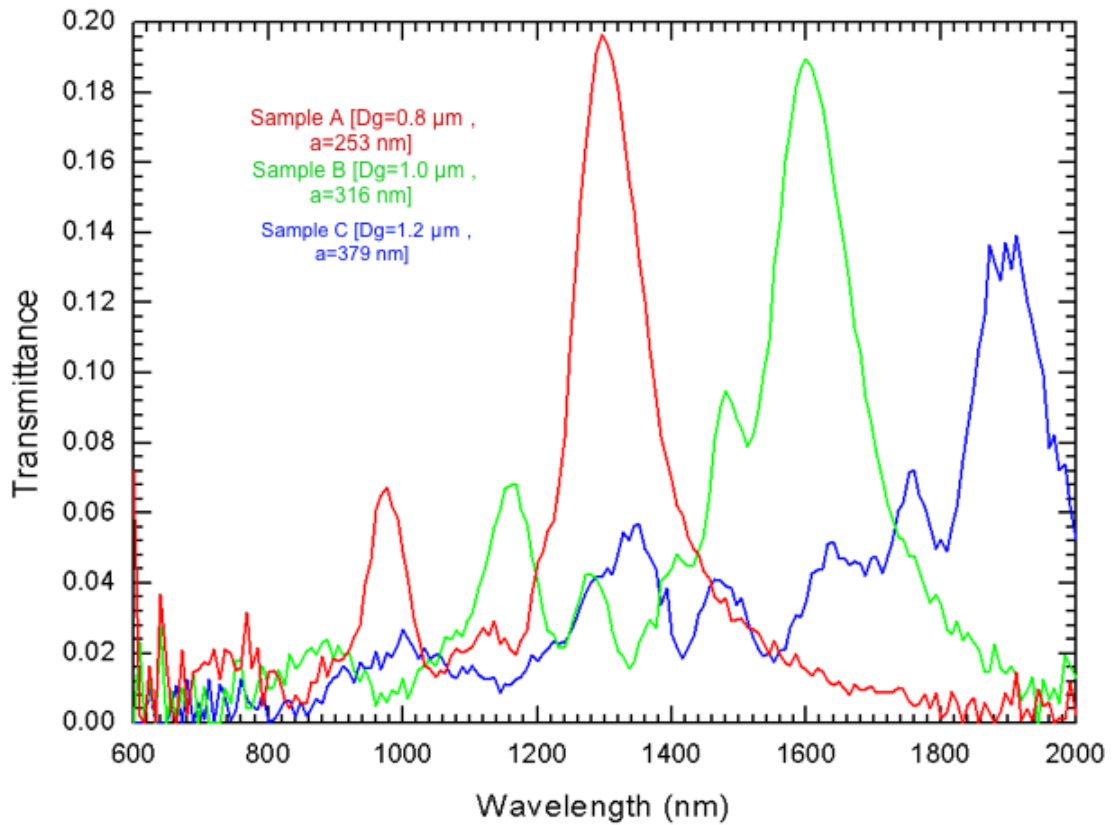


Figure 5: Transmittance intensity using 10x magnification of NIR wavelengths of sample entirely covered with PMMA, Figure 2(e).

The theory of trapped electromagnetic modes uses diffraction thresholds to explain the wavelength position of the enhanced transmission peaks. The theory states that diffraction thresholds exist near characteristic wavelengths and it is here that the electromagnetic field gets trapped in the holes. These trapped fields slowly decay by emitting quasi-monochromatic radiation. (The radiation is emitted over wavelengths spanning the transmission maximum.)

We used the equation  $l_s \lambda_s = n_d D_g$  to calculate the characteristic wavelengths of the diffraction thresholds for all three samples. Our calculations are shown in Table II, where  $n_d=1.4$  is the refractive index of our substrate material,  $D_g$  is the lattice spacing of the sample, and  $l_s=(l_x^2 + l_y^2)^{1/2}$ .  $l_x$  and  $l_y$  can only be integers meaning  $l_s$  can take the values of 1,  $\sqrt{2}$ ,  $\sqrt{5}$ , etc. Figs. 6 and

Table II: Calculated diffraction threshold wavelengths,  $\lambda_s$ , for each sample.

Sample	Diff. Threshold ( $l_s=1$ )	Diff. Threshold ( $l_s=\sqrt{2}$ )
A	1159 nm	822 nm
B	1529 nm	1025 nm
C	1728 nm	1300 nm

7 show the calculated characteristic wavelengths for the diffraction thresholds, indicated by color coded arrows, over-plotted onto the transmittance intensity graphs when the sample had no PMMA on it (Fig. 6) and when the sample was spin-coated with a layer of PMMA (Fig. 7). The calculated diffraction thresholds do not perfectly match the experimental results because the calculation does not take into account the index of refraction for material above the film.

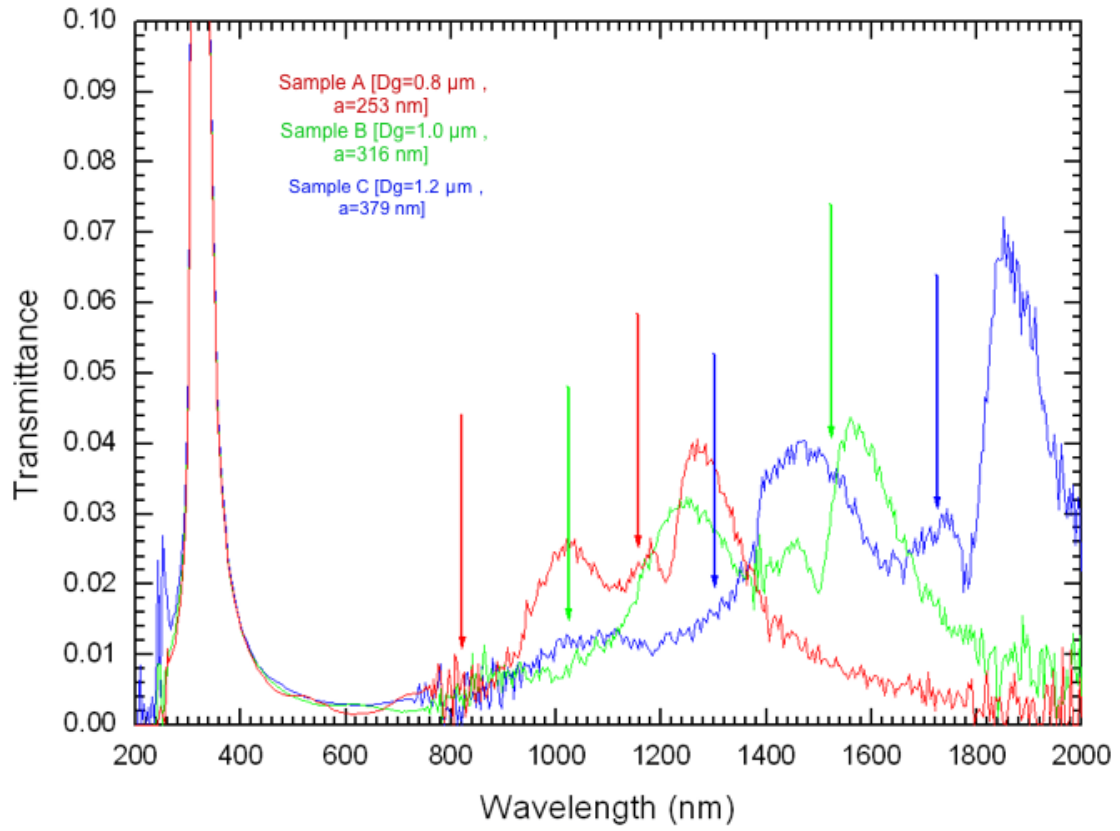


Figure 6: Transmittance intensity for all three arrays with no PMMA. Arrows indicate the calculated diffraction thresholds,  $l_s=1$  and  $l_s=\sqrt{2}$ , for each sample with  $n_d=1.4$ .

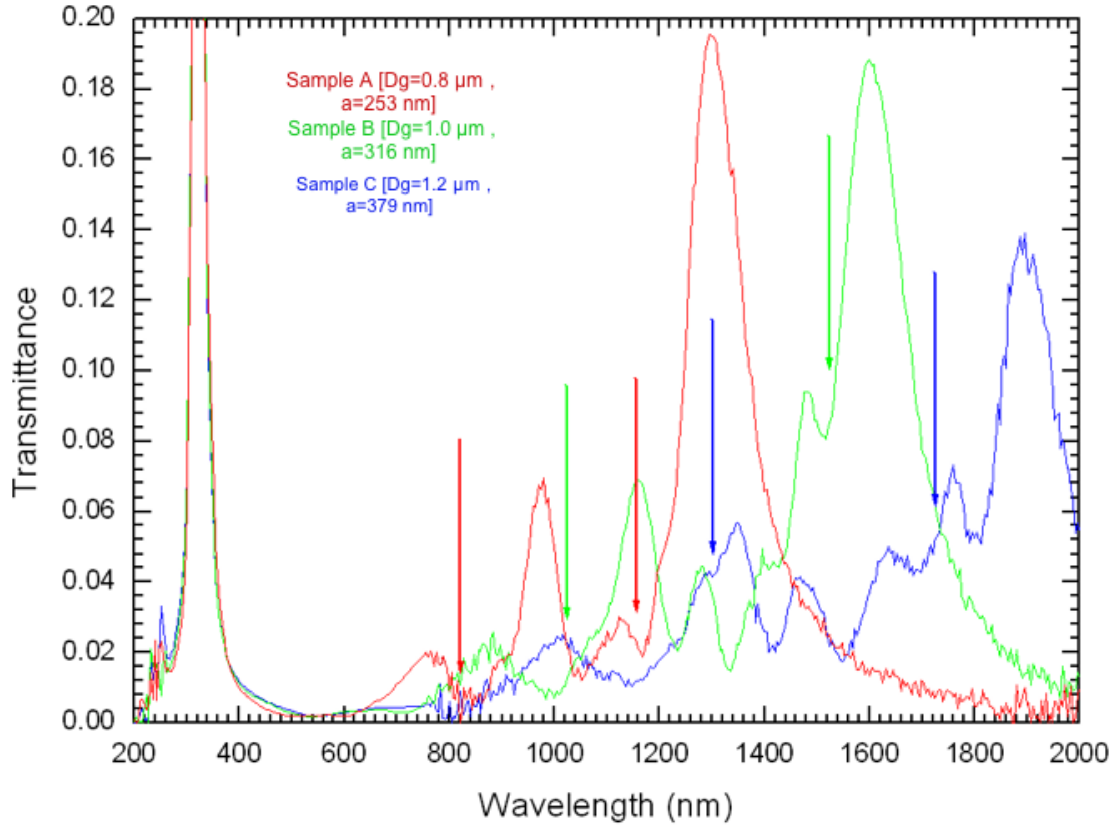


Figure 7: Transmittance intensity for all three arrays coated with PMMA. Arrows indicate the calculated diffraction thresholds,  $l_s=1$  and  $l_s=\sqrt{2}$ , for each sample with  $n_d=1.4$ .

## Conclusion

Our results matched our expectations in that sample A with the smallest hole size and closest lattice spacing had its transmittance peak at the short-

est wavelength, and sample C with the largest hole size and biggest lattice spacing had the longest wavelength for its transmittance intensity peak for all three conditions. We measured enhanced transmission peaks of almost twice the open area fraction of 10% when the refractive index of the material above and below the silver film differed by approximately 0.1. The transmittance intensity peaked at only 0.044% when the refractive indices above and below the material differed by 0.5. In the future we hope to further investigate more samples with smaller lattice spacing and hole size using a new preparation technique, as well as other metal films including gold.

## Acknowledgments

I would like to thank Dr. Tanner for giving me the chance to work in his lab, Dr. Ingersent, Kristin Nichola, and Dr. Hershfield for organizing this REU program, and the NSF for their financial support. I would also like to thank Dimitrios Koukis for his guidance and patience.

## References

- [1] T.W. Ebbesen, H.J. Lezec, H. F. Ghaemi, T. Thio, and P. A. Wolff, *Nature* **391**, 667 (1998).
- [2] H.A. Bethe, *Phys. Rev.* **66**, 163 (1944).
- [3] K. Woo, Ph.D. dissertation, University of Florida, 2006.

- [4] S. Selcuk, K. Woo, D. B. Tanner, A. F. Hebbard, A. G. Borisov, S.V. Shabanov, *Phys. Rev. Lett.* **97**, 067403 (2006).
- [5] Technical data sheet of Microposit S1800 series photo resists (Shipley, marlborough, Massachusetts, May 2006).
- [6] C. A. Ordal et. al., *Appl. Opt.* **22**, 1099 (1983).